ROLE OF INORGANIC PHOSPHATE IN VESICLE RELEASE FROM OSTEOGENIC CELLS

by

Victoria Smethurst

B.S. Biology, Florida State University, 2015

Submitted to the Graduate Faculty of

The School of Dental Medicine in partial fulfillment

of the requirements for the degree of

Master of Science

University of Pittsburgh

2018

UNIVERSITY OF PITTSBURGH

School of Dental Medicine

This thesis was presented

by

Victoria Smethurst

It was defended on

July 19th, 2018

and approved by

Dr. Elia Beniash, Professor, Department of Oral Biology,

Dr. Juan Taboas, Assistant Professor, Department of Oral Biology

Thesis Director: Dr. Dobrawa Napierala, Associate Professor, Department of Oral Biology

Copyright © by Victoria Smethurst

2018

Role of Inorganic Phosphate in Vesicle Release from Osteogenic Cells

Victoria Smethurst, B.S.

University of Pittsburgh, 2018

Extracellular vesicles (EV) are membrane-enclosed microstructures released from the cell. EV can transport cargo—such as DNA, RNA, and proteins—into the extracellular space and act as a form of intercellular communication. Matrix vesicles (MV) are a unique type of EV produced by mineralizing cells. In previous studies, utilizing *in vitro* models of pre-odontoblasts and vascular smooth muscle cells, it was determined that phosphate induces the release of MV and alters MV composition. We hypothesized that elevated phosphate alters the composition of MV through the alteration of gene expression. To determine whether this hypothesis holds true or not, 17IIA11 cells, a pre-odontoblast cell line, were exposed to elevated phosphate for 24h, 48h, and 72h. RNA and MV were then collected for further analysis. Using nanoparticle tracking analysis, we determined that the size distribution of the MV was not altered by the phosphate. Next, to evaluate a possible mechanism driving MV composition change, we compared the effect of phosphate on gene expression to the effect of phosphate on MV composition. No correlation was identified between changes in gene expression and changes in MV composition. These findings suggest that phosphate does not alter the composition of MV through altered gene expression. Future studies should focus on other mechanisms that may drive MV composition changes.

TABLE OF CONTENTS

LIST OF TABLES

LIST OF FIGURES

PREFACE

First, I would like to thank my family for their love and support throughout this process of getting my master's degree. Next, I would like to thank my mentor, Dr. Dobrawa Napierala, for her patience and guidance. I would also like to thank my fellow lab members for their support: Daisy Monier, Dr. Sana Khalid (in part, whose work I based my thesis on), and Dr. Mairobys Socorro. I would also like to thank Drs. Juan Taboas and Elia Beniash, for their knowledge, insights and support as members of my dissertation committee. I'm grateful for the Graduate Student Research Award (GSRA) from the Dean's office and Department of Oral Biology, School of Dental Medicine at the University of Pittsburgh.

For providing me with guidance and the basis for my thesis work, I would like to thank Dr. Sandeep Chaudhry. For everyday advice and encouragement, as well as general lab expertise, I would like to thank Kristi Rothermund.

For technical support in Cryo-EM, I would like to acknowledge Dr. James Fredrick Conway and Alexis Huet. For technical support for NTA, I would like to acknowledge Dr Yoel Sadovsky and Hui Li.

Finally, I would like to thank all the members of the CCR and the Oral Biology graduate students; your support and friendship have meant so much to me. Truly, thank you for your kindness and friendship.

1.0 INTRODUCTION

1.1 EXTRACELLULAR VESICLES

Extracellular vesicles (EV) are membrane-enclosed microstructures released from the cell. EV can transport cargo—such as DNA, RNA, and proteins—into the extracellular space and act as a form of intercellular communication. All cells release EV and, the cargo of EV often retains its biological function. There are several types of EV, characterized based on their biogenesis or release pathways; the most well-defined types of EV are apoptotic bodies, exosomes, microvesicles (Figure 1) (György, Szabó et al. 2011, Yuana, Sturk et al. 2013, Colombo, Raposo et al. 2014, Yanez-Mo, Siljander et al. 2015, Zaborowski, Balaj et al. 2015, Hasegawa 2018). Apoptotic bodies are released after the initiation of apoptotic cell death. This type of EV involves blebs directly from the plasma membrane with a diameter ranging in size from 500 nanometers (nm) to 1 micrometer (µm). Exosomes, another commonly studied EV subtype, are formed through the fusion of multivesicular bodies containing smaller vesicles and the plasma membrane, which results in the release of the smaller vesicles (exosomes) ranging in diameter from 40nm to 120nm. A third EV subtype, microvesicles, bud directly from the plasma membrane, contain cytoplasmic cargo, and range in diameter from 50nm to 1 µm (Roberts, Stewart et al. 2004, Thery, Amigorena et al. 2006, Julien, Khoshniat et al. 2009, György, Szabó

et al. 2011, Yuana, Sturk et al. 2013, Colombo, Raposo et al. 2014, Yanez-Mo, Siljander et al. 2015, Zaborowski, Balaj et al. 2015, Bottini, Mebarek et al. 2018).

Current research in the field suggests that the function of EV is related to the composition of the cargo. An early study by Théry et al. (2001) evaluating the composition of EV released from dendritic cells established the first extensive protein map of an EV population, showing that the composition of vesicles released by dendritic cells could impart an immunostimulating function (Théry, Boussac et al. 2001). This study suggests that EV act as a form of cell-cell communication.

Other studies of EV have theorized that the roles of EV are far more varied than previously thought. For example, EVs have been found to contain and carry the receptors of many growth factors, such as TNF-α, EGF, and FGF. The extracellular matrix (ECM) retains these growth factors, and they can be released during ECM remodeling. The release of these molecules can regulate cell proliferation, migration, and morphogenesis. EV containing the receptors for these factors suggest that they may play a role in regulating their release. EVs have also been found to contain matrix metalloproteinases with proteolytic activity and EV may play a role in alteration of EV content and ECM degradation (Rackov, Garcia-Romero et al. 2018). These findings indicate the diverse roles EV can play in cellular function.

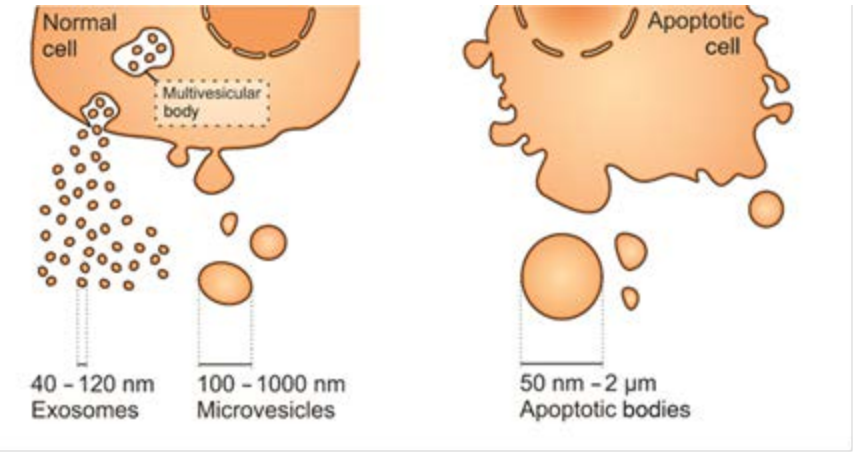

Figure 1. Extracellular vesicles (EV) are produced by cells and vary by type.

Exosomes and microvesicles are produced from both healthy and diseased cells, whereas apoptotic bodies are produced by cells undergoing apoptosis. Adapted from Zaborowski et al. 2015

1.2 MATRIX VESICLES

In bone biology, we find a fourth well-defined type of EV: matrix vesicles (MV). These range in size from approximately 80nm to 220nm and bud from specific regions of the plasma membrane. MV are a unique set of EV that anchor to the ECM and initiate the mineralization of the ECM through the nucleation of hydroxyapatite. They are known to be released from mineralizing cells such as hypertrophic chondrocytes and osteoblasts. Furthermore, EV derived from arterial endothelial cells, vascular smooth muscle cells, and macrophages have been associated with the pathological mineralization of the arteries, a dangerous complication of cardiovascular diseases. (Anderson 1967, Boyan, Schwartz et al. 1989, Wuthier and Lipscomb 2011, Shapiro, Landis et al. 2015, Chaudhary, Kuzynski et al. 2016, Bottini, Mebarek et al. 2018, Chaudhary, Khalid et al. 2018, Hasegawa 2018).

The composition of MV released from stem cells undergoing osteogenic differentiation (using an osteogenic medium composed of an inorganic phosphate (P_i) source and ascorbic acid)

has been previously studied. These MV were shown to be enriched in the proteins involved in mineralization such as tissue non-specific alkaline phosphatase (TNAP), calcium phosphate transporters, and annexesins (calcium transporters). These vesicles are also enriched in ESCRT (endosomal sorting complexes required for transport) proteins, suggesting they are packaged and sorted through the endosomal pathway before being released into the ECM (Thouverey, Malinowska et al. 2011).

Studies of cartilage and arteries have also identified MV as being associated with pathological mineralization. However, one study comparing the proteomes of MV released from normal and osteoarthritic cartilage found that only a small number of proteins, mostly involved in inflammation, were different between the two groups (Rosenthal, Gohr et al. 2011). Another study evaluating MV from normal cartilage samples identified full-length mRNA contained in MV for collagen II, aggrecan, and ANKH, an inorganic pyrophosphate transport regulator. When chondrocytes were then exposed to these MV, the MV were internalized, and there was an observed change in gene expression by these genes (Mitton, Gohr et al. 2009).

While the composition of MV released from osteoblasts, chondrocytes, and cartilage has been evaluated, our group was the first to evaluate the composition of MV released from odontoblasts, which undergo physiologic mineralization, as well as vascular smooth muscle cells, which undergo pathologic mineralization. From these studies, we identified P_i as an initiator of MV release from these cells (Figure 2) (Anderson, Garimella et al. 2005, Yuana, Sturk et al. 2013, Chaudhary, Kuzynski et al. 2016, Chaudhary, Khalid et al. 2018).

1.3 PHOSPHATE AND MINERALIZATION

Pi is one of the most important and abundant ions present in the body. It is part of the DNA backbone, stores energy in the form of ATP, and activates enzymes through phosphorylation. It is a major component of hydroxyapatite and, most importantly for our study, acts as a signaling molecule, particularly in the initiation of mineralization (2006, Khoshniat, Bourgine et al. 2011, Chaudhary, Kuzynski et al. 2016, Chaudhary, Khalid et al. 2018).

Elevated P_i is provided, in part, to the cell locally through conversion of pyrophosphate to P_i by TNAP, and it signals for osteogenic differentiation of stem cells (Ciancaglini, Yadav et al. 2010, Wuthier and Lipscomb 2011, Millan 2013, Huesa, Houston et al. 2015, Fakhry, Roszkowska et al. 2017). Unpublished data from our lab has indicated that Runt-related transcription factor 2 (Runx2), the master regulator of osteogenic differentiation, is up-regulated by elevated Pi in a pre-odontoblast cell line (data not shown), suggesting that Pi may regulate osteogenic differentiation through alteration of gene expression. Furthermore, a study utilizing MC3T3-E1 cells (a pre-osteoblastic cell line) showed significant modulation of protein expression, specifically in functions related to cell cycle regulation, proliferation, and DNA synthesis, when exposed to elevated Pi (Conrads, Yi et al. 2005).

Several studies have also identified alteration of gene expression of proteins related to mineralization when osteogenic progenitor cells and osteosarcoma cells were exposed to elevated P_i. These proteins include osteopontin (OPN), and dentin matrix protein 1 (DMP1) (Beck, Zerler et al. 2000, Beck, Moran et al. 2003, R. 2003, Conrads, Yi et al. 2005, Khoshniat, Bourgine et al. 2011). In an unpublished RNA-seq analysis of 17IIA11 cells (17A, a pre-odontoblast cell line) exposed to elevated Pi, we identified significant alteration of gene expression of genes known to be involved in the mineralization of the ECM (data not shown).

This finding provides further evidence supporting Pi's role as a signaling molecule involved in mineralization.

However, very little is understood about the pathways through which Pi acts. The only known mediators of phosphate signaling include Extracellular signal-regulated kinase 1 and 2 (ERK1/2). Members of the P_i transporter (PiT) family are the only known transporters of P_i into the cell. Of further interest to this study is the fact that many of the proteins known to regulate local concentrations of phosphate (TNAP, PiT-1) are known to be enriched in MV (Beck, Zerler et al. 2000, Beck, Moran et al. 2003, R. 2003, Conrads, Yi et al. 2005, Julien, Khoshniat et al. 2009, Khoshniat, Bourgine et al. 2011, Wuthier and Lipscomb 2011, Bottini, Mebarek et al. 2018). Another intriguing observation is that the protein products of genes affected by elevated P_i are known to reside in the ECM during mineralization and are important regulators of mineralization (DMP1 and OPN) (McKee and Nanci 1996, Beck, Zerler et al. 2000, R. 2003, Khoshniat, Bourgine et al. 2011, Chaudhary, Khalid et al. 2018). As P_i acts as a signaling molecule, and many regulators of P_i and mineralization are enriched in MV, we decided to investigate whether P_i played a role in MV composition and release from osteogenic cells and found that it did (Figure 2).

1.4 PHOSPHATE AND EXTRACELLULAR VESICLE RELEASE FROM OSTEOGENIC CELLS

MV have long been thought to be the nucleation sites of hydroxyapatite crystals (Wuthier and Lipscomb 2011, Alves, Eijken et al. 2014, Chaudhary, Kuzynski et al. 2016, Bottini, Mebarek et al. 2018, Chaudhary, Khalid et al. 2018, Hasegawa 2018). In previous work, we evaluated the

role of P_i in the stimulation of MV release. Using the 17IIA11 (17A) cell line, we determined that P_i was responsible for the increased MV production (Figure 2A.). We also determined that the EV collected from the ECM possibly contained amorphous hydroxyapatite suggesting they are mineralization competent (Chaudhary, Kuzynski et al. 2016). Furthermore, when we exposed a vascular smooth muscle cell line (MOVAS) to elevated P_i, we observed an increase in MV release after 72h(Figure 2B) (Chaudhary, Khalid et al. 2018). These two studies confirmed the importance of P_i for induction of mineralization and led to new questions about how these MV are produced, what their function may be, and how P_i alters them.

Once we established that P_i induces MV release, we wanted to investigate whether the protein composition of the MV released from both 17A and MOVAS cells was altered due to P_i. We did this because it is thought that the composition of EV (of which MV is a subset) is thought to reflect their function. From our literature review, we also found that previous studies collected MV from both the medium and ECM of cultured cells for evaluation. However, we hypothesized that these vesicle populations would have different functional roles from each other and therefore varied compositions. As a result, we decided to evaluate them separately. Using mass spectrometric analysis, we determined that elevated Pi exposure alters the protein composition of EV from both the medium and ECM in 17A (unpublished, Figure 3A) and MOVAS cells (Figure 3B) (Chaudhary, Khalid et al. 2018).

From our previous findings, we hypothesized that elevated P_i alters the composition of MV through alteration of the gene expression of odontoblasts.

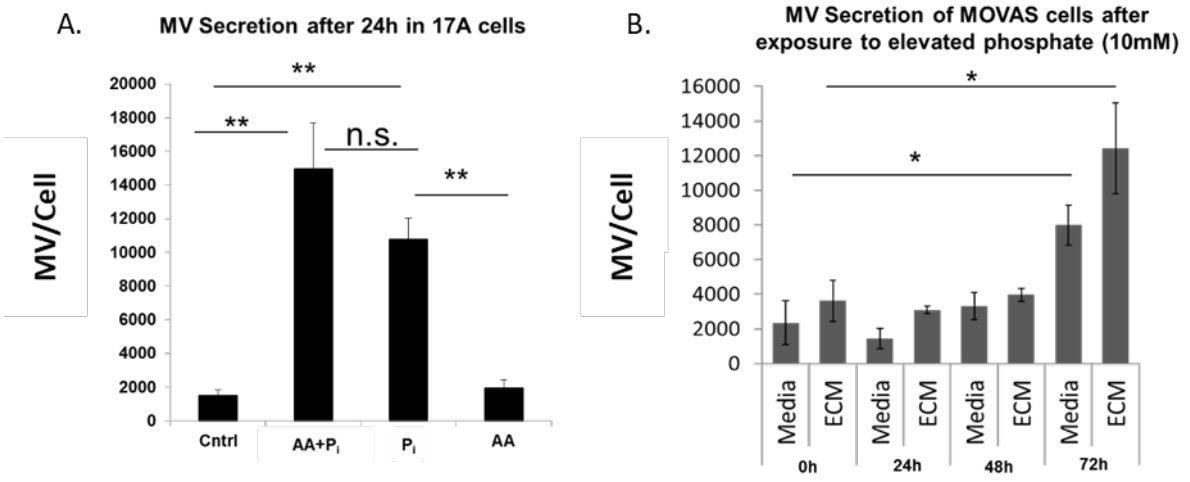

Figure 2. Phosphate induces extracellular vesicle release from mineralization-competent cells.

A. Comparison of the number of MV released by cells within 24h of stimulation with standard osteogenic medium (ascorbic acid and P_i; AA + P_i), 10 mM Na-Pi buffer (P_i), or ascorbic acid (AA), with cells cultured in standard growth medium (Cntrl). Data are represented as the mean values of three independent experiments ± SD, *$p<0.05$ and **$p<0.005$. B. Results of nanoparticle tracking analyses show the number of EVs isolated from conditioned medium (medium) or extracellular matrix (ECM) of MOVAS cells grown in the presence of 10 mM P_i for 24, 48 and 72h. Data are represented as the mean values of three independent experiments ± SD, *$p<0.01$. Adapted from (Chaudhary, Kuzynski et al. 2016)

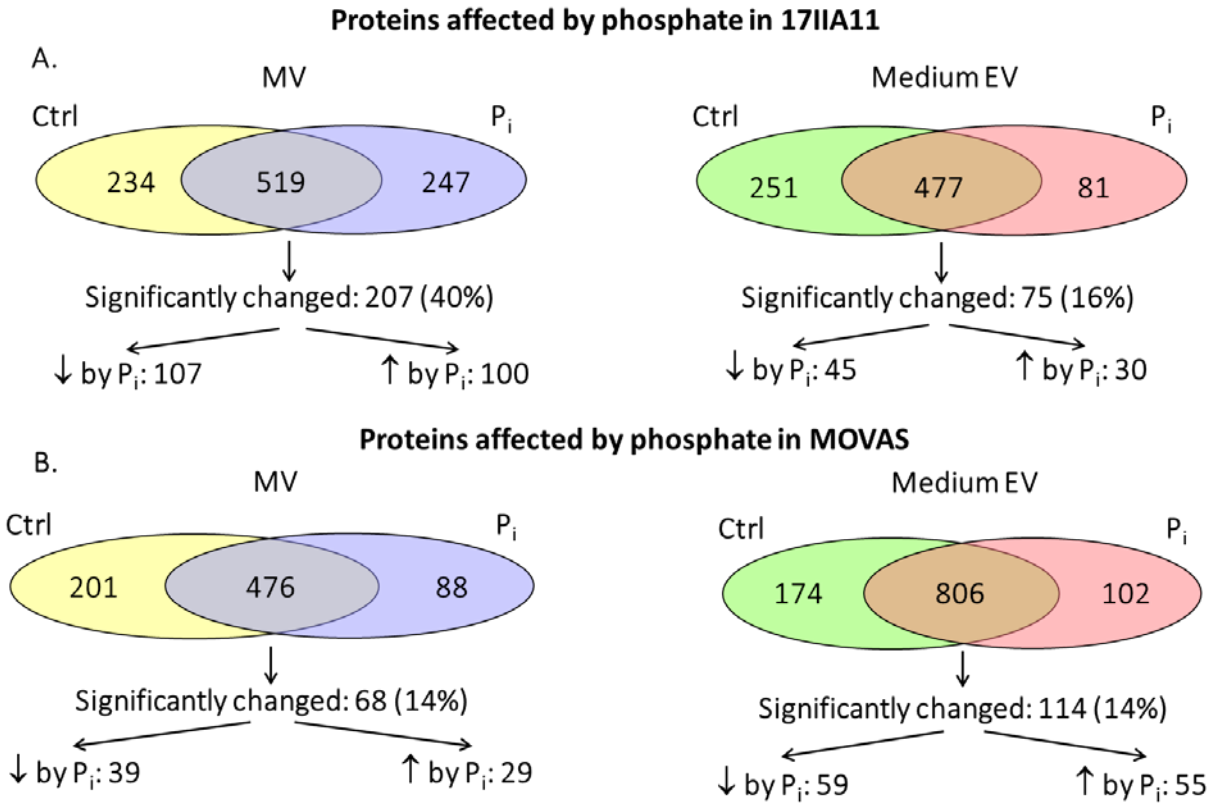

Figure 3 Phosphate alters protein composition of EV from 17A and MOVAS cells

Summary of proteomic analyses of EVs released from MOVAS cells under standard growth conditions (Ctrl) and upon 24 h treatment with 10 mM Pi (Pi). EVs were isolated either from conditioned medium (medium) or from the extracellular matrix (ECM). **A.** Venn diagrams summarizing the effect of high Pi on EV protein composition of EV released from 17IIA11 (17A) cells **B.** Venn diagrams summarizing the effect of high Pi on EV protein composition released from MOVAS cells. Adapted from (Chaudhary, Khalid et al. 2018).

2.0 OBJECTIVE OF STUDY

Matrix vesicle (MV) release is odontoblasts has been under-studied. Most studies evaluate MV in the context of later stages of chondrogenesis or osteogenesis and without identification of the factor that stimulates the release of these vesicles. In our previous study, we identified P_i as the driver of an early MV release from a pre-odontoblast cell line and vascular smooth muscle cell line. Furthermore, we determined that elevated P_i exposure alters both the vesicle composition and the gene expression of osteogenic cells. Considering these observations, the objective of this study is to determine if alteration of gene expression is a mechanism through which vesicle composition is altered.

3.0 MATERIALS AND METHODS

3.1 CELL LINES

The 17IIA11 (17A) is a mouse pre-odontoblast cell line generated by Priam et al (2005). 17A were maintained in Dulbecco's Modified Eagle Medium supplemented with 5% fetal bovine serum (FBS) and 100 units/ml penicillin and 100 ug/ml streptomycin. This cell line was maintained at 37ºC and at 5% carbon dioxide.

The MOVAS cell line is a mouse aortic smooth muscle cell line obtained from the ATCC. It was maintained in Dulbecco's Modified Eagle Medium (DMEM) supplemented with 10% FBS and 100 units/ml penicillin and 100 µg/ml streptomycin (Cellgro, Manassas, VA). This cell line was maintained at 37 ºC and at 5% carbon dioxide.

3.2 EXPERIMENTAL DESIGN

3.2.1 Exome-Depleted Fetal Bovine Serum Preparation

FBS was diluted to a concentration of 20% with DMEM supplemented with 100 units/ml penicillin and 100 µg/ml streptomycin (Cellgro, Manassas, VA). The FBS solution was centrifuged at 100,000 rpm in an ultracentrifuge for 14h to deplete vesicles from the FBS. The

FBS was then filter sterilized using Nalgene™ Rapid-Flow™ with 0.2 µm pores (Thery, Amigorena et al. 2006).

3.2.2 Experimental Conditions

17A and MOVAS cells were plated at 10 million cells per 10 cm dish in exome-depleted medium for 24 to 48h before treatment. DMEM was supplemented with exome-depleted FBS to a final concentration of 10% FBS exome-depleted medium for the 17A cell line and 20% FBS exome-depleted medium for the MOVAS cell line. High FBS concentrations were used to account for FBS loss during the exome depletion process.

For the experimental conditions, the medium was then further supplemented with 10mM sodium phosphate buffer (NaP_i), the P_i source (pH 7.4) ($NaH_2PO_4 \cdot H_2O$ and Na_2HPO_4) (as it has been shown that NaP_i is a more controlled and direct source of P_i) or ultra-pure water. The cells were then grown for 24h, 48h, and 72h for vesicle collection. After 48h the medium was replenished. Medium and ECM derived vesicles were then collected from the 24h group and from the ECM only at 48h and 72h groups. In all other experiments, 5% FBS (for 17A cells) and 10% FBS (for MOVAS cells) was used in place of exome-depleted FBS.

3.3 ISOLATION OF VESICLES

3.3.1 Medium-derived matrix vesicles

The medium MV was collected from the culture dish and centrifuged at 2,000g for 20min; the supernatant was then ready for further purification or stored in a 4ºC fridge for up to a week or in a -80ºC fridge indefinitely.

3.3.2 Matrix-derived extracellular vesicles

Once the medium was removed from the culture plate, the vesicles were released from the extracellular matrix (ECM) using enzymatic digestion. Specifically, For 17A cells DMEM was supplemented with 2.5 mg/ml collagenase IA (Sigma, St Louis, MO) and 2mM calcium chloride and added to the culture plates for 2h at 37ºC and 5% carbon dioxide for 17A cells. For MOVAS cells, 1 mg/ml of collagenase IA was used, and elastase (0.8U/ml) was also added to release matrix vesicles from MOVAS ECM.

Each mixture was then centrifuged for 20 min at 2000g, and the supernatant was immediately ready for further purification or storage in a 4ºC fridge for up to a week or in an 80ºC fridge indefinitely.

3.4 PURIFICATION OF VESICLES

All vesicles were purified using several steps of ultracentrifugation. First, the Medium and ECM collections were centrifuged at 4ºC 10,000g for 30min to remove any cellular debris. The resulting supernatant was then transferred to clean tubes and centrifuged at 4ºC at 100,000g for 1.5h to 3h. Next, the supernatant itself was discarded, and the pellet remaining after centrifuging was resuspended in PBS or Tris-buffered saline (TBS) (50 mM Tris–HCl, pH 7.4 and 154 mM NaCl) and centrifuged at 4ºC at 100,000g for 70 min. The supernatant was again removed, and the remaining pellet was dissolved in PBS or TBS for further analysis and stored at -80ºC (Thery, Amigorena et al. 2006).

The protein concentration of the vesicles was evaluated using a Pierce™ BCA Protein Assay Kit (Thermo Fisher Scientific), and its color quantification was evaluated using a Synergy™ H1 microplate reader (BioTek, Vermont, USA)

3.5 QUALITATIVE AND QUANTITATIVE EVALUATION OF THE PREPARATION QUALITY OF EXTRACELLULAR VESICLES

3.5.1 Cryo-electron microscopy

Vesicles suspended in TBS were applied to holey carbon film (Quantifoil Micro Tools) and vitrified in liquid ethane using an FEI Vitrobot Mark IV. The grids were transferred to a Gatan 626 cryo-sample holder and imaged in an FEI Tecnai F20 electron microscope operated at 200

kV and nominal magnifications ranging from 32,750x to 65,500x. Low-dose images were captured with a Gatan Ultrascan 4000 CCD camera.

3.5.2 Nanoparticle tracking analysis

The size and concentration of the purified vesicles were determined by Nanoparticle Tracking Analysis (NTA) using NanoSight NS300 (Malvern Instruments Ltd, Worcestershire, UK). Data acquisition and analysis were performed using NTA 2.3 Analytical Software. One video file of 60 seconds at camera level 10 from each sample was created. A detection threshold limit of 10 was used to analyze the size and concentration of the vesicles.

The percentage of the vesicles in the size range of interest was determined by adding the number of particles within the size range of interest and dividing by the total number of particles.

3.5.3 Silver staining of proteins

Samples were prepared using 1x NuPAGE™ LDS buffer and 1x NuPAGE™ Sample reducing agent (Thermo Fisher Scientific). They were boiled for 10 min and incubated on ice for 5 min. These samples were also used for the western blot analysis. The vesicle proteins (5µg) were separated by SDS-PAGE electrophoresis using NuPAGE™ 4-12% Bis-Tris Protein Gels (Thermo Fisher Scientific) at 200V for 1h.

A Pierce™ Silver Stain Kit was used as instructed to stain the gel. A new sliver stain was done for each new vesicle preparation.

3.5.4 Western blotting

After the vesicle samples were prepared as described in the sliver staining section, the vesicle proteins (7.5µg) were separated by SDS-PAGE electrophoresis using NuPAGE™ 4-12% Bis-Tris Protein Gels and transferred onto a nitrocellulose membrane. Specific proteins were detected with primary antibodies against: TNAP (1:1000; R&D Systems), GLG1 (1:1000; Sigma), OPN (1:10000; R&D Systems), and PIAD3 (1:1000 Proteintech). Signals were detected using a horseradish peroxidase-conjugated secondary antibody and an enhanced chemiluminescence detection kit (ECL; Amersham Biosciences, Pittsburgh, PA, USA). All secondary antibodies (GE Healthcare or Fisher) were used at 1:3000 dilution (ani-rabbit, anti-rat, and anti-goat).

3.6 DETERMINING WHETHER PHOSPHATE-INDUCED GENE EXPRESSION CHANGES IN 17A CELLS CORRELATE WITH AN ALTERATION IN MV COMPOSITION

3.6.1 RNA isolation from total lysate of 17A cells

Total RNA was extracted using a GenElute Mammalian Total RNA Miniprep Kit (Sigma Aldrich, St. Louis, MO, USA). The total RNA (1 µg), after DNase I treatment (Life Technologies, Grand Island, NY, USA), was converted to cDNA using a SuperScript III Reverse Transcriptase Kit (Life Technologies, Grand Island, NY, USA) and diluted in a ratio of 1:10 with ultra-pure water for further analysis.

3.6.2 Reverse transcription polymerase chain reaction

Gene expression analyses were performed using a StepOnePlus™ Real-Time PCR System (Thermo Fisher Scientific) and Fast SYBR Green reaction mix (Roche, Indianapolis, IN, USA). The primer sequences were (F denotes forward primer, R denotes reverse primer):

Akp2-F	CAGTGGGAGTGAGCGCAGCC
Akp2-R	GCACTGGGTGTGGCGTGGTT
Dmp1-F	GCTGGGTCACCACCACCACC
Dmp1-R	GGAGGGTCCTCCCCACTGTCC
Opn-F	ATGAGGCTGCAGTTCTCCTGG
Opn-R	AAAGCTTCTTCTCCTCTGAGCTGCC
Ank-F	CACCCTGATAGCCTACAGTGAC
Ank-R	GGAAGGCAGCGAGATACAGG
Phospho1-F	ATGAGCGGGTGTTTTCCAGC
Phospho1-R	GGTCTTCAACACATCTTCAGC
mPanx3-F	ACCCCCATGTCTTCTGGGAT
mPanx3-R	GTAGGTGGCCACTAGCCAAT
PTHR1-F	ACTGTGGCAGATCCAGATGC
PTHR1-R	AATCTCTGCCTGCACCTCAC
Slc13a5-F	GTCGAGGGAAACACCGTTCA
Slc13a5-R	TTGGGCGACTTTCCAATCCA
Itga6-F	CACTCAGGTTCGAGTGACGG
Itga6-R	CAGCCTTGTGATAGGTGGCAT
Cdsn-F	AATGTCCAGCCCGGCATAA

Cdsn-R	GGTCCCAATGCTCTTAGCCA
Itga6-F	GCTGTTCTTGCCGGGATTCT
Itga6-R	ATGCATCGGAAGTAAGCCTCT
Sema7a-F	GGGTGAGGGAGACAGGGGAGAGCGAAGA
Sema7a-R	CCTCCTTCAAAATGACCACGGCAAAT

Expression was normalized to GAPDH expression, and relative expression was determined through comparison to the average control at the corresponding time point (ex: 48h control was compared to 48h P_i).

3.6.3 Statistical analysis

The vesicles were collected and pooled from ten 10cm dishes. RNA was collected from 3 controls, and 3 P_i treated 17IIA11 cells. Data are presented as the mean +/- standard deviation. Probability values were calculated using a Two-Tailed *t*-test, where $p \leq 0.05$ (*), $p \leq 0.01$ (**), and $p \leq 0.001$ (***) were considered to be statistically significant.

4.0 RESULTS

4.1 QUALITATIVE AND QUANTITATIVE EVALUATION OF THE PREPARATION QUALITY OF EXTRACELLULAR VESICLES

4.1.1 Shape of vesicles and quality of preparation based on Cryo-EM

4.1.1.1 Shape and quality of extracellular vesicles collected from MOVAS cells

EV are spherical membrane-enclosed particles. For our study, we were interested in vesicles ranging in size from 50nm to 220nm, as this size range contains MV (Chaudhary, Kuzynski et al. 2016, Chaudhary, Khalid et al. 2018). To evaluate the purity of the vesicles collected during the process described above, cryo-electron microscopy was performed on MOVAS cells.

Vesicles were collected from MOVAS cells from either the medium or ECM and after elevated P_i exposure for 24h. Four groups were evaluated: Control EV-Medium, P_i EV-Medium, Control EV-ECM, and P_i EV-ECM. The Cryo-EM images showcased in Figure 4 demonstrate vesicles within the size range of approximately 50 to 120nm (indicated by white arrows). From the images, we can conclude that the vesicles collected using the ultracentrifugation method reside within the MV range of interest (50nm to 220nm) and are relatively pure, as indicated by the lack of significant contamination by other particles. This is especially true of the ECM groups, as ECM contamination by ECM collagen fibrils is absent.

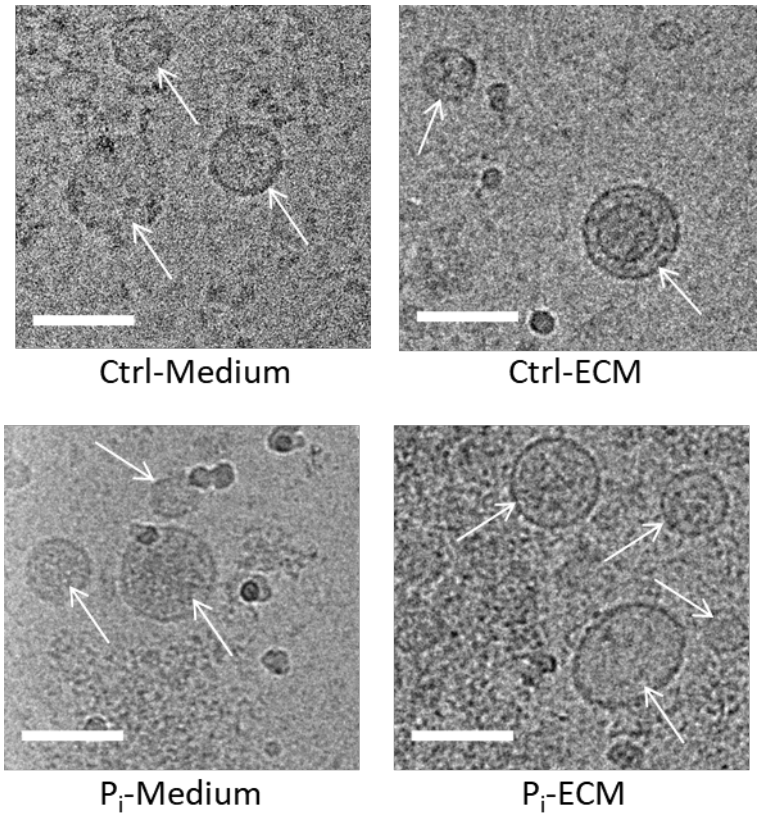

Figure 4. Cryo-EM of extracellular vesicles (EV) released by MOVAS cells

Cells were grown in standard conditions (Ctrl) or with 10mM phosphate (P_i). Vesicles were collected from ECM and medium after 24h. Scale bars are 100nm. Adapted from (Chaudhary, Khalid et al. 2018).

4.1.2 Verification of mass spectrometric analysis

Further analysis of the proteins detected by mass spectrometry was done to validate the mass spectrometric analysis of the 17A cells, which was only performed once. To determine the quality of this analysis, we attempted to evaluate several proteins that were detected in MV using mass spectrometric analysis by using a western blot analysis on new samples. We evaluated the same four groups used for mass spectrometry analysis (Control MV-Medium (Crtl-med), Phosphate MV-Medium (P_i-med), Control MV-ECM (Ctrl-ECM), Phosphate MV-ECM (P_i-ECM)). Of all the proteins detected, we chose proteins based on their detection from the mass spectrometric analysis. For example, some proteins were present in all samples, some only in the ECM group (ECM), some only in the medium (med) group; meanwhile, other proteins showed significant alterations by phosphate, both increase and decrease presence in vesicles. Unfortunately, of the 14 proteins tested, only 2 were detectable by western blot. This could be due to poor antibodies or an insufficient amount of protein present to be detectable.

Golgi Glycoprotein 1 (Glg1) and Protein Disulfide Isomerase Family A Member 3 (Piad3) were the two proteins detectable by western blot. The mass spectrometric data showed a significant increase by elevated P_i in the ECM group, and we saw the same pattern using western blot analysis (Figure 5A). Silver staining of gels using the same vesicle preparation was used as a loading control. Of note from the silver stain is the different banding pattern in the vesicles collected from the medium and ECM (Figure 5B). This further confirms, after mass spectrometric analysis, that the MV collected from the medium and ECM are different vesicle populations.

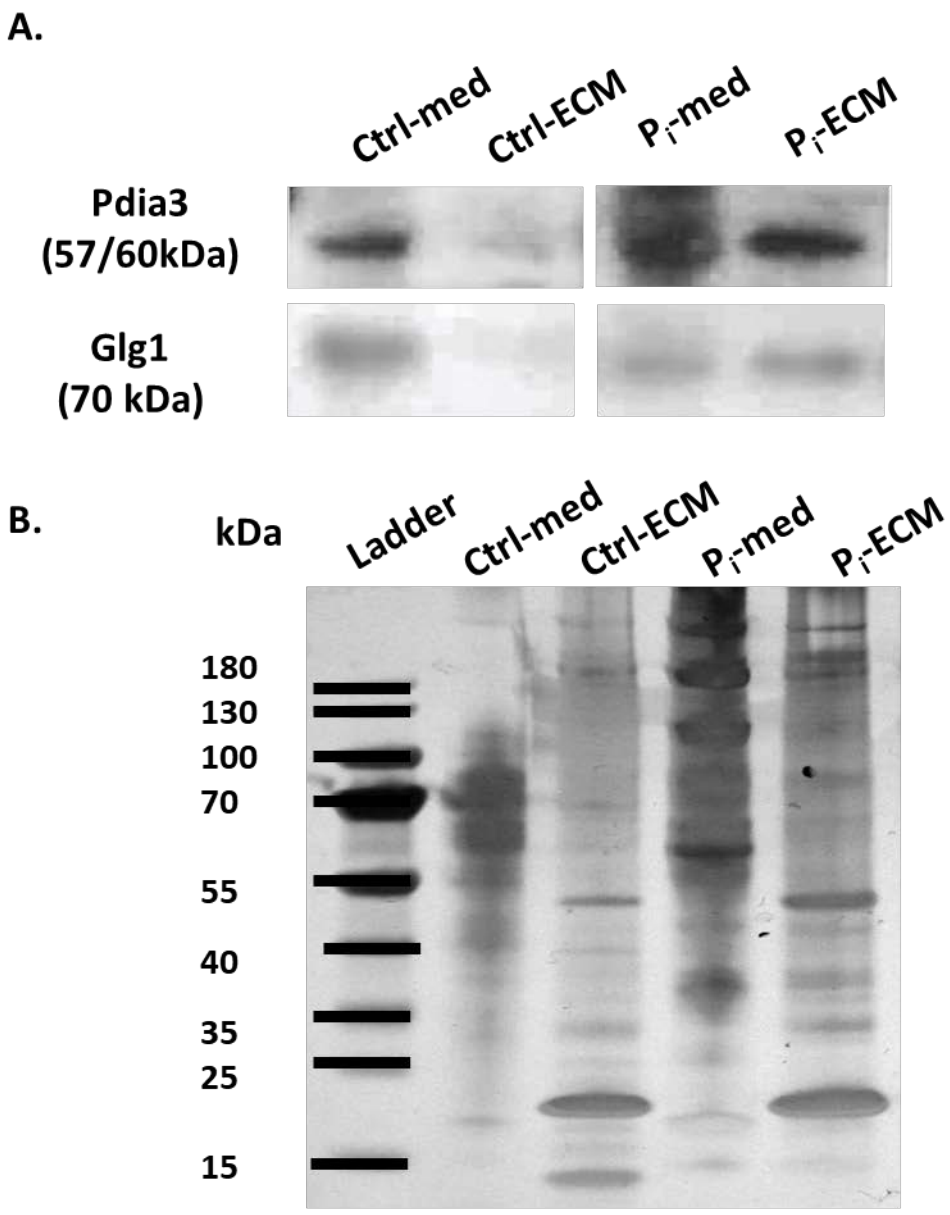

Figure 5. Western blot analysis of proteins in MV released by 17IIA11 cells into the medium (med) or ECM after 24h of elevated phosphate exposure.

A.Western blot of MV detecting Pdia3 and Glg1. 7.5ug of protein/lane. B. Silver stain of gel. 5ug of protein/lane. This does not seem to be correct formatting – please check

4.1.3 Size distribution analysis of ECM vesicles based on nanoparticle tracking analysis

From the mass spectrometric analysis and the silver staining of MV proteins, we determined that the vesicles isolated from the ECM are significantly different from those isolated from the medium. Next, we focused on the ECM-derived vesicles to determine the role of phosphate in MV biogenesis. Vesicle biogenesis pathway effects the size of the EV released, the biogenesis pathway for exosomes, which are formed in the cell and released through exocytosis, results in vesicles that range in size from approximately 50nm to 80nm. On the other hand, apoptotic bodies, which are released during apoptosis, range in size from approximately 500nm to 1µm (Yuana, Sturk et al. 2013, Yanez-Mo, Siljander et al. 2015, Zaborowski, Balaj et al. 2015, Bottini, Mebarek et al. 2018). As vesicle isolation results in a heterogeneous population of vesicles, it is important to verify if the isolation method results in the collection of MV. If size distribution is altered, it may be due to a change in the biogenesis pathway. We evaluated the MV released from 17A cells into the ECM over 72h after exposure to 10mM P_i. This resulted in 6 groups being used for further study: 24H Control ECM MV (24H C ECM), 24H P_i ECM MV (24H P ECM), 48H Control ECM MV (48H C ECM), 48H P_i ECM MV (48H P ECM), 72H Control ECM MV (72H C ECM), and 72H P_i ECM MV (72H P ECM).We assessed the size distribution of MV using nanoparticle tracking analysis to determine if P_i alters vesicle size distribution.

4.1.3.1 Evaluating extracellular vesicle preparation using nanoparticle tracking analysis

The vesicle size range of interest to this study is between 50nm to 220nm, which includes exosomes (50nm to 79nm in size) and matrix vesicles (80 nm to 220 nm in size). For the purpose of our study, we strictly classified the vesicles collected based on size; it should be noted that

these are the approximate size ranges of exosomes and MV respectively. Particles smaller than 50nm are most likely small protein aggregates or small pieces of cellular debris. Larger particles may be protein clumps, large pieces of cellular debris that weren't removed, or apoptotic vesicles.

Our vesicle preparations were between 73% and 88% vesicles of interest (Table 1.) This is similar to preparations done in our lab previously (Chaudhary, Kuzynski et al. 2016).

Table 1. Nanoparticle Tracking Analysis of MV released from 17IIA11 cells

Sample	Mean Sample Size	Mode Sample Size	Percent of Sample Sized between 50 and 80nm (Exosomes)	Percent of Sample Sized Between 80 and 220nm (Matrix Vesicles)	Total Preparation in Range of Interest (50nm to 220nm)
24 H C ECM	96nm	59nm	28%	47%	75%
24H P ECM	97nm	75nm	25%	53%	78%
48H C ECM	129nm	104nm	18%	70%	88%
48H P ECM	121nm	71nm	24%	59%	83%
72H C ECM	127nm	70nm	18%	55%	73%
72H P ECM	145nm	89nm	16%	64%	80%

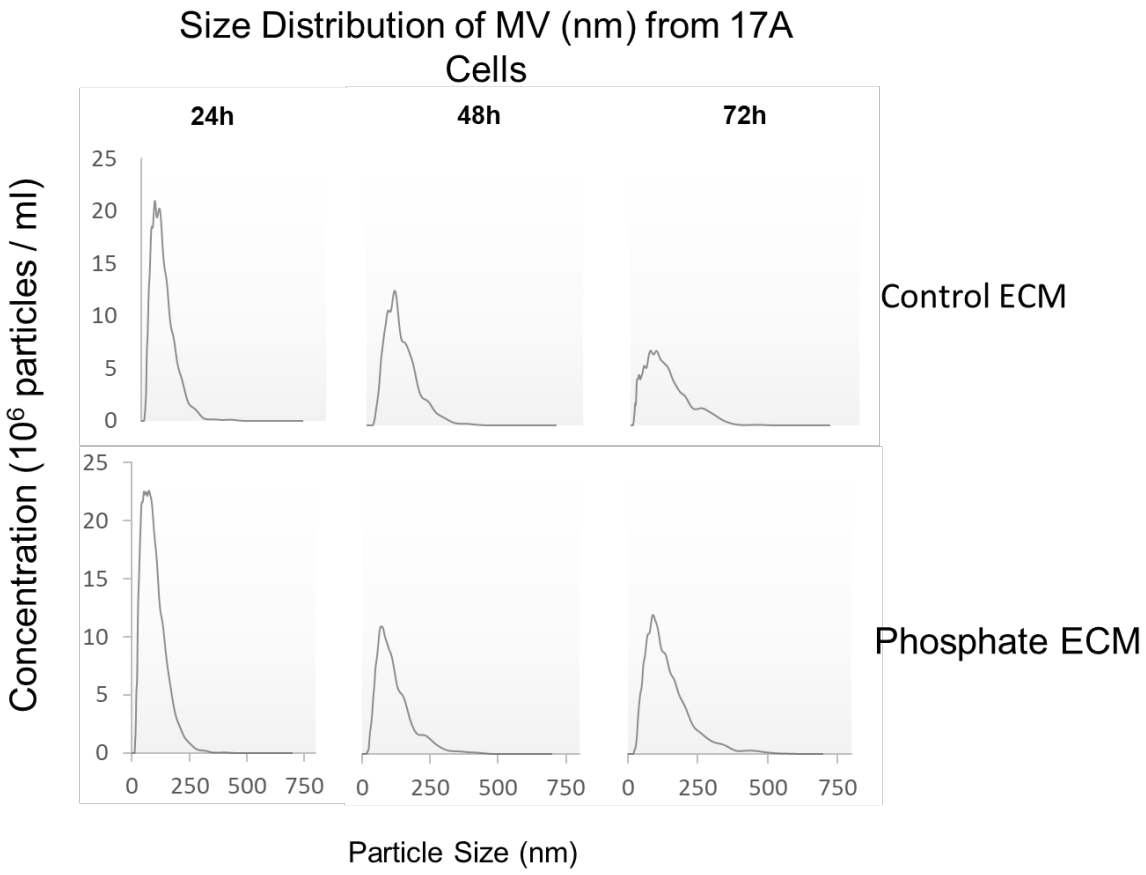

Figure 6. Size distribution of EV collected from 17IIA11 cells.

Cells were grown under standard growth conditions (Ctrl) or with 10 mM Pi (Pi). EVs were isolated from the extracellular matrix (ECM) after 24, 48, and 72h. Vesicle preparations were evaluated using nanoparticle tracking analysis. The graphs demonstrate the size distribution of particles contained within the samples. Again – check to see how much info should be here under the figure.

4.1.3.2 Comparing extracellular vesicles released from 17IIA11 cells grown in elevated Phosphate Conditions

Although P_i exposure has been shown to alter the composition of MV, the mechanism through which this alteration occurs is unknown. One-way P_i may alter vesicle composition is through alteration of vesicle biogenesis. We used nanoparticle tracking analysis to determine if the size of the vesicles changed in response to elevated P_i. Using the nanoparticle tracking data, we evaluated the size distribution of MV between treated and non-treated groups at the same time point.

We did not identify differences in size distribution between the control and P_i groups at each time point. Comparing the mean particle size of control at and P_i groups at 24h, we found that it was 96 and 97nm, respectively. The mean particle size of control at 48h and P_i at 48h was 129 and 121nm, respectively. A larger difference in mean particle size was observed between the control at 72h and P_i at 72h groups, 127 and 145nm, respectively, however, this difference is due to increased contamination by particles larger than 220nm, not due to an increase in average vesicle size (Table 1 and Figure 6) .

4.1.3.3 Comparing extracellular vesicles released from 17IIA11 cells grown in elevated phosphate conditions over time

To determine if MV size changed over time in response to elevated P_i, we used the nanoparticle tracking data to analyze the size distribution of vesicles released by 17A cells over time, from 24h of elevated P_i exposure to 72h of elevated P_i exposure. We did not identify differences in size distribution within the vesicle groups collected from the ECM over time.

In the 24h P_i group, the mean particle size was 97nm, and the mode size of the particles detected was 75. After 48h the mean particle size increased to 121nm, but the mode particle size was only

71nm. Further, after 72h, the mean particle size increased to 145nm, but the mode particle size only increased to 89. These changes are in the lower range of MV size and are not meaningfully different. However, as this experiment was only performed once, statistical significance could not be ascertained. (Table 1 and Figure 6). The increasing mean identified here can be explained by an increase in the number of contaminating particles over 220nm the longer treatment continues. The mode particle size of each sample is the size of particle most commonly detected. This does not shift meaningfully as the experiment progresses. This indicates that the pathway producing the vesicles is still the same, even though the mean is increasing.

4.2 DETERMINING WHETHER PHOSPHATE-INDUCED GENE EXPRESSION CHANGES IN 17A CELLS CORRELATE TO AN ALTERATION IN MV COMPOSITION

In an unpublished RNA-seq analysis, we determined that elevated P_i alters the gene expression of 17A cells. Many of the genes affected are known to be involved in the mineralization of the ECM (TNAP, Dmp1, and Opn). P_i also induces the release of MV, the nucleation sites of hydroxyapatite(Chaudhary, Kuzynski et al. 2016).As we have shown that exposure to elevated P_i alters the composition of MV, we wanted to determine if some of the alterations in MV composition we identified were due to the alteration of gene expression.

Genes were chosen for examination based on at least one of four criteria (genes selected based on the criteria stated are listed in ()): alteration in expression in response to P_i as indicated by RNA-seq analyses (all genes selected for analysis),presence in MV as indicated by our mass spectrometry analysis (*Dmp1, Opn, Itag6, Akp2, Pth1r, Panx3, Slc13a5, Cdsn*), presence in EV based on the literature (*Itga6, Sema7a, TNAP, Panx3, and Slc13a5* (Thouverey, Malinowska et al. 2011)), or function (all genes selected for analysis).

4.2.1 Determination if P_i induced MV composition change is related to P_i-induced gene expression changes (increased expression).

Osteopontin (*Opn*) is a non-collagenous protein present in the extracellular matrix (ECM) of mineralized tissue (McKee and Nanci 1996). Elevated Pi significantly increases the expression of Opn in 17A cells after 24h ($p \leq 0.001$), and increased expression was continued for 72h ($p \leq 0.05$) (Figure 7). A small number of particles of *Opn* were detected in the medium and the ECM vesicles after exposure to Pi by mass spectrometry analysis, but this was not replicated in the western blot analysis (Figure 8, and Table 2). The detected levels of Opn in the mass spectrometry analysis were at low levels, which may not have been sufficient for detection by western blot. There was also a significant amount of background, which may have obscured the signal.

Progressive ankylosis protein (*Ank*) is a transmembrane protein that transports inorganic pyrophosphate from the intercellular space into the ECM. Loss of this protein in mice has been shown to decreased bone mass (Kim, Minashima et al. 2010, Wuthier and Lipscomb 2011). In

our study, *Ank* showed a significant increase in gene expression at 24h ($p \leq 0.001$) and 48h ($p \leq 0.05$) after P_i exposure (Figure 7). Ank was not detected in the matrix vesicles (Table 2).

Dentin matrix phosphoprotein 1 (*Dmp1*) is another protein that localizes to the ECM; it is responsible for nucleating hydroxyapatite (Wu, Teng et al. 2011). Elevated P_i significantly increased expression of *Dmp1* in 17A cells after 24h ($p \leq 0.001$), and this increased expression was maintained for 72h ($p \leq 0.05$) (Figure 7). A small number of particles of Dmp1 were detected in medium vesicles after exposure to P_i (Table 2).

Integrin alpha 6 (*Itga6*) is a cell-surface adhesion receptor that binds to the ECM and mediates cell–ECM interactions (Wang, Choi et al. 2014, Yanez-Mo, Siljander et al. 2015). Elevated P_i significantly increased the expression of Itga6 in the 17A cells after 24h ($p \leq 0.001$), and the increased expression was maintained for 48h ($p \leq 0.05$) (Figure 7). It was detected in the vesicle groups: Cntrl-Medium EV, P_i –Medium EV, and P_i –ECM MV, but there was no significant alteration by P_i (Table 2).

Semaphorin 7A (*Sema7a*) is a GPI-anchored membrane glycoprotein, and mutations of this gene have been implicated in reduced bone mineral density (Delorme, Saltel et al. 2005). *Sema7a* was not detected in matrix vesicles, even though it showed a significant increase in expression after 24h ($p \leq 0.01$) and maintained the significant increase in expression at 72h ($p \leq 0.05$) (Figure 7 and Table 2).

Dual Specificity Phosphatase 6 (*Dusp6*) is a cytosolic MAP kinase phosphatase that specifically recognizes and inactivates the ERK1/2, a known mediator of P_i signaling. In a previous study, a Dusp6 mutant mouse showed dwarfism and coronal craniosynostosis (Bradshaw and Dennis 2010). Dusp6 was not detected in the matrix vesicles, even though it showed a significant increase in expression after 24h ($p \leq 0.01$) and maintained increased expression for 48h ($p \leq 0.05$) (Figure 7 and Table 2).

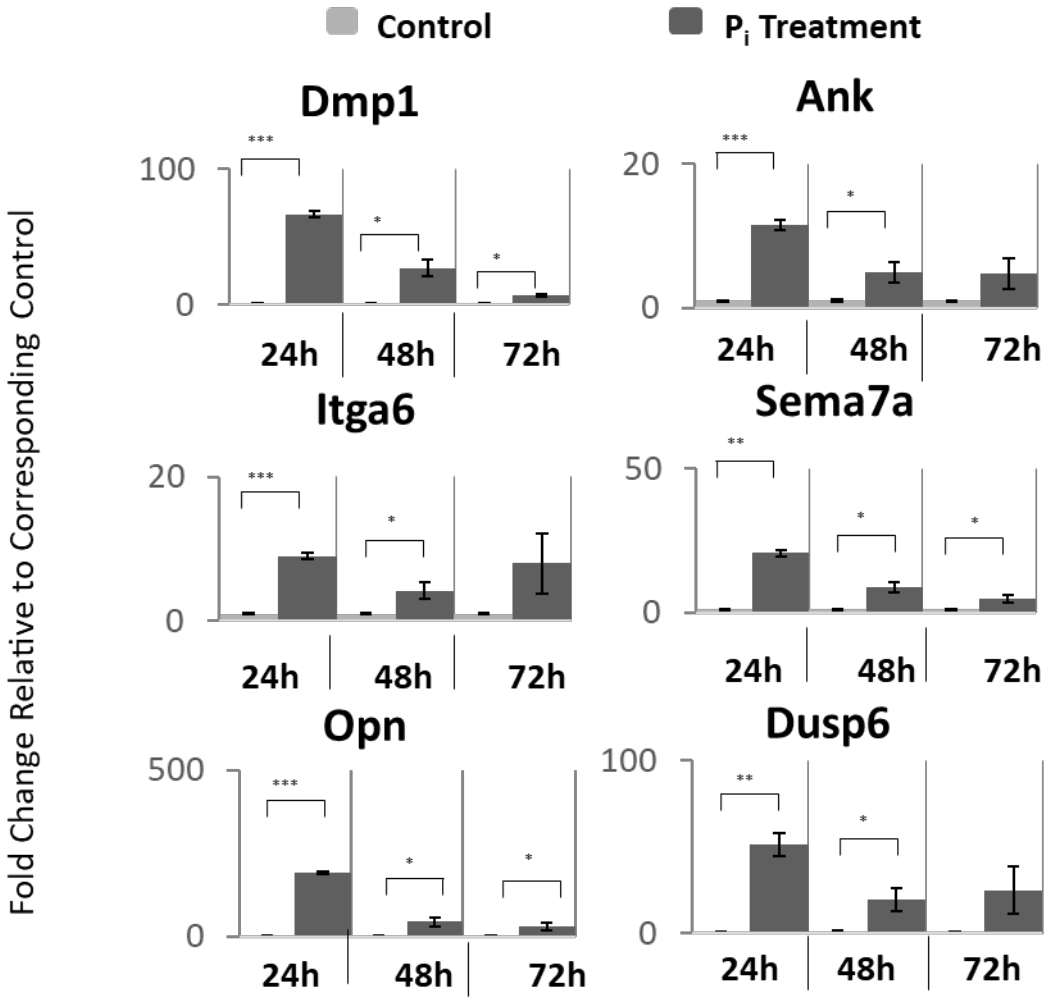

Figure 7. Analysis of upregulated genes in 17A cells after exposure to elevated P_i

RNA from 17IIA11 cells were collected under standard growth conditions (Control) at 24h, 48h, 72h and upon 24h,48h, and 72h after treatment with 10 mM P_i (P_i). Fold change for the phosphate treated groups was determined relative to control, which was set at 1. $p \leq 0.05$ (*), $p \leq 0.01$ (**), and $p \leq 0.001$ (***).$p \leq 0.05$ (*), $p \leq 0.01$ (**), and $p \leq 0.001$ (***).

Table 2. Detection pattern in MV of genes upregulated by P_i using mass spectrometry

Gene	Detection of Protein in MV after 24h P_i exposure (17A)
Dmp1	P_i –Medium EV
Ank	No detection
Opn	P_i –Medium EV P_i –ECM MV
Itag6	Cntrl-Medium EV P_i –Medium EV P_i –ECM MV *No significant alteration by Pi*
Sema7a	No detection
Dusp6	No detection

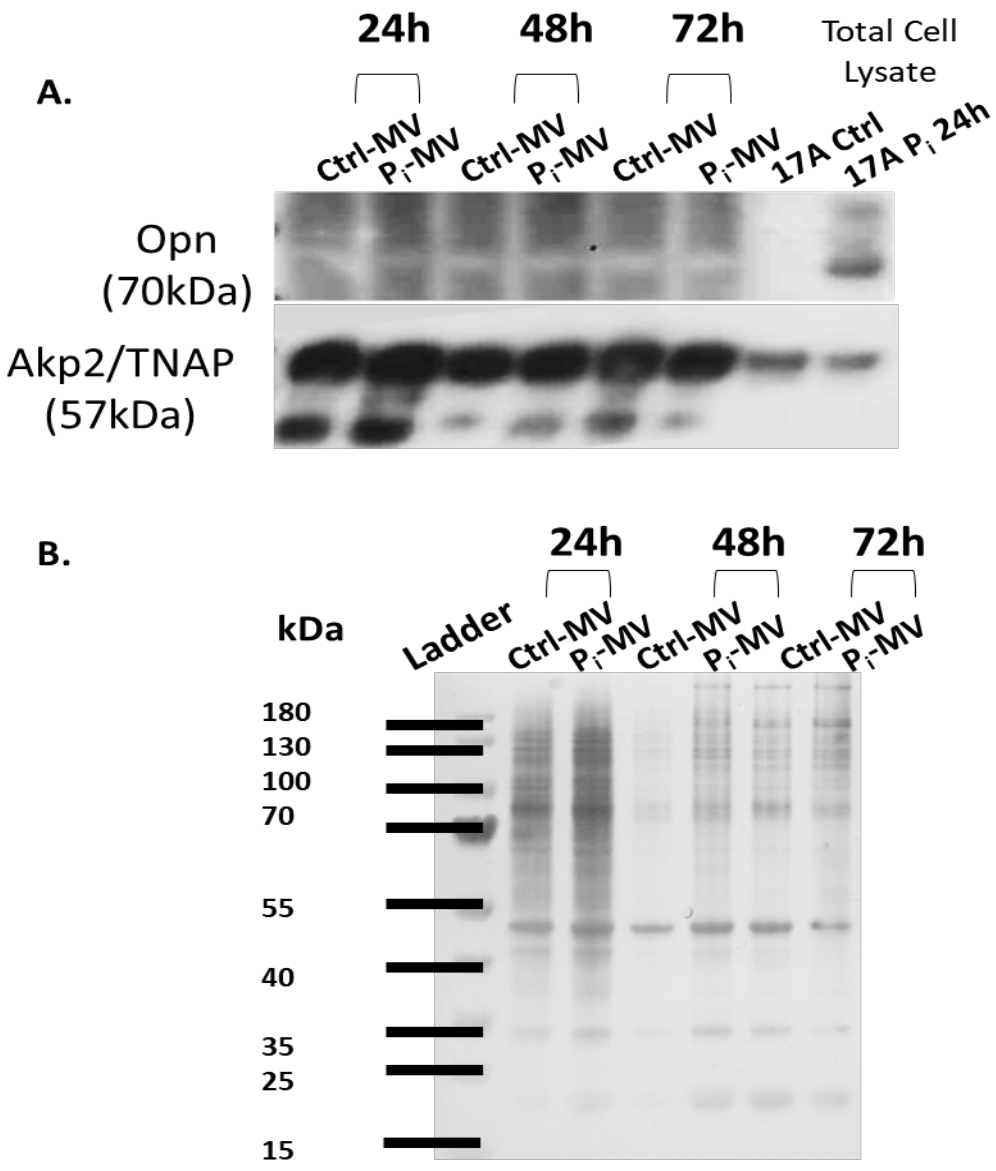

Figure 8. Western blot analysis of proteins in MV released into the ECM from 17IIA11 cells after 72h of elevated P_i exposure.

A. Western blot analysis of Opn and Akp2/TNAP. MV loaded at 7.5ug/lane and total cell lysate at 10ug protien/lane. B. Silver stained gel of MV from the same preparation as those prepared for western blot 5ug protein/lane were loaded.

4.2.2 Determination if Pi induced MV composition change is related to Pi-induced gene expression changes (decreased expression).

Tissue non-specific alkaline phosphatase (*Akp2/TNAP*) is a membrane protein that converts pyrophosphate to P_i. Mutations in *AKP2* lead to a condition called hypophosphatasia, where bone mineralization is severely impaired (Ciancaglini, Yadav et al. 2010, Wuthier and Lipscomb 2011, Huesa, Houston et al. 2015). At 24h, 48h and 72h of elevated P_i exposure, Akp2 showed a significant decrease in expression using qRT-PCR ($p \leq 0.05$, $p \leq 0.01$, and $p \leq 0.05$, respectively) (Figure 9). Akp2 was detected in all vesicle groups, but no significant change in Akp2/TNAP was detected by mass spectrometry or western blot (Figure 8 and Table 3).

Phosphoethanolamine/Phosphocholine Phosphatase (*Phospho1*) is a member of the haloacid dehalogenase superfamily. It is involved in MV-mediated mineralization. It plays a role in savaging P_i within the MV lumen to promote hydroxyapatite formation. Phospho$^{-/-}$ mice have shown decreased mineral density among other skeletal abnormalities (Roberts, Stewart et al. 2004, Ciancaglini, Yadav et al. 2010, Huesa, Houston et al. 2015). Over 24h and 48h, *Phospho1* showed a significant decrease in expression using qRT-PCR ($p \leq 0.05$, and $p \leq 0.01$, respectively) (Figure 9). It was not detected in MV (Table 3). This shows that it was never trafficked into the MV and, therefore, its decreased expression does not affect MV composition.

Parathyroid hormone 1 receptor (*Pth1r*) is the receptor for the parathyroid hormone. It is a transmembrane protein that is part of the regulatory pathway that maintains phosphate and calcium homeostasis. Several human diseases with bone and dental phenotypes are associated with mutations in *PTH1R*, such as Blomstrand's lethal chondroplasia, and Familial primary failure of tooth eruption (Cheloha, Gellman et al. 2015, Fan, Bi et al. 2016). *Pth1r* showed a

significant decrease in expression after 24h ($p \leq 0.01$) and 48h ($p \leq 0.05$) (Figure 9). It was only detected in the control vesicles at a low level (Table 3).

Pannexin 3 (*Panx3*) is a protein involved in cell-cell and cell-matrix communication. Mice lacking Panx3 have shown delayed and disorganized mineral deposition (Oh, Shin et al. 2015, Ishikawa and Yamada 2017). After 24h of P_i exposure, *Panx3* showed a significant decrease in expression ($p \leq 0.001$) as well as at 48h ($p \leq 0.05$) and 72h ($p \leq 0.01$) using qRT-PCR (Figure 9). It was present in all 17A released extracellular vesicles (EV) and showed no significant alteration by P_i (Table 3).

Solute Carrier Family 13 Member 5 (*Slc13a5*) is a sodium-dependent citrate transporter. Up to 70% of citrate is stored in bone, and citrate helps stabilize and nucleate hydroxyapatite crystals. Slc13a5$^{-/-}$ C57BL/6 mice have shown decreased bone mineral density and impaired bone formation, along with impaired enamel formation (Irizarry, Yan et al. 2017). Slc13a5 showed a significant decrease in expression over 24h ($p \leq 0.01$) and 48h ($p \leq 0.01$) using qRT-PCR (Figure 9). *Slc13a* was present at a low level in the control vesicle groups but not in the vesicles treated with Pi (Table 3).

Corneodesmosin (*Cdsn*) is an extracellular matrix/cell adhesion molecule (Xiao, Camalier et al. 2007). After 24h of P_i exposure, it showed a significant decrease in expression ($p \leq 0.05$) as well as at 48h ($p \leq 0.01$) and 72h ($p \leq 0.05$) using qRT-PCR (Figure 9). In the mass spectrometry analysis, it was only detected in the P_i-MV group, but at low levels (Table 3). This finding is contrary to the gene expression analysis, indicating that the decrease in *Cdsn* mRNA does not affect its trafficking into the MV.

In summary, when gene expression changes are compared to MV composition, the changes do not appear to correlate to MV composition after 24h of P_i exposure. Furthermore, analysis by western blot of Opn and TNAP in MV does not show a correlation to gene expression.

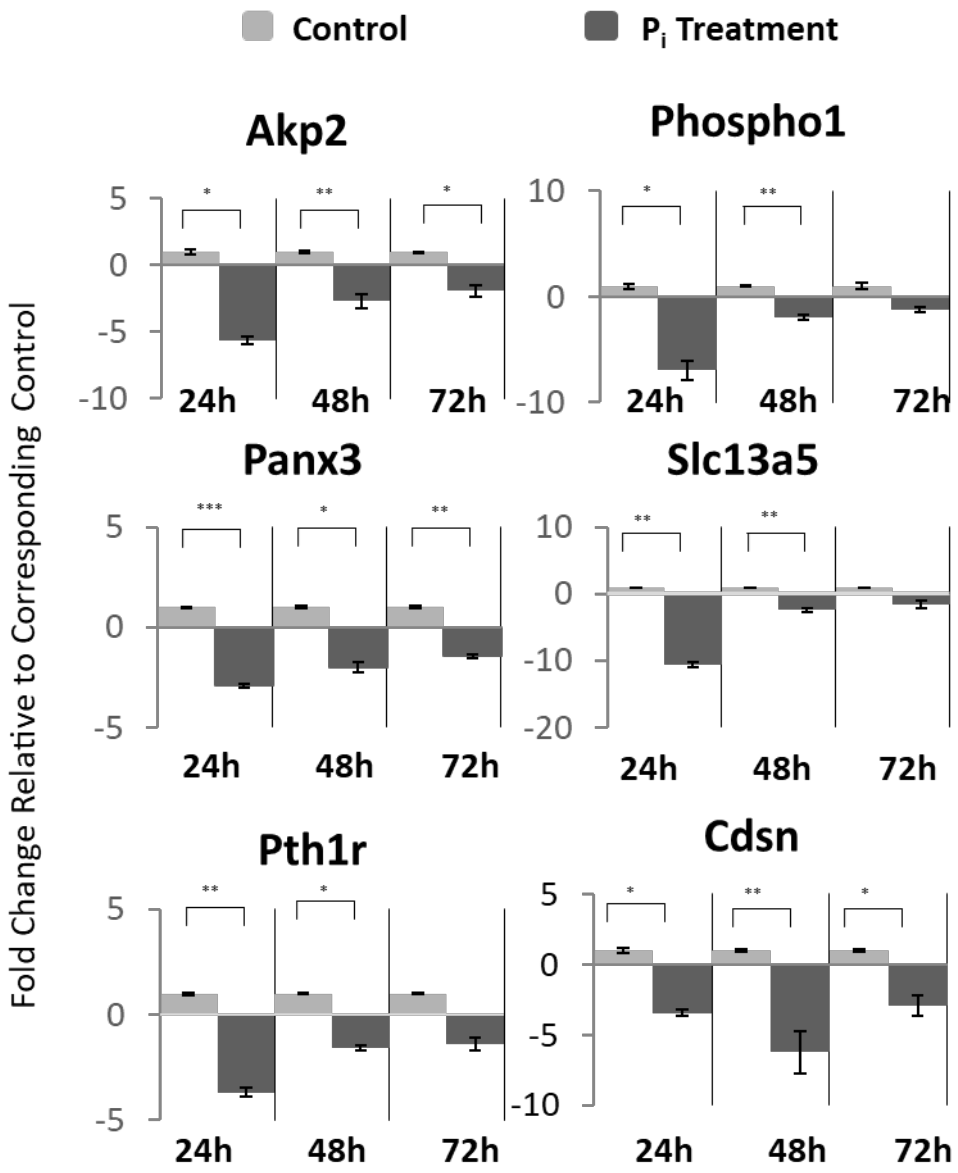

Figure 9 Analysis of downregulated genes in 17A cells after exposure to elevated Pi

RNA from 17IIA11 cells were collected under standard growth conditions (Control) at 24h, 48h, 72h and at 24h,48h, and 72h after treatment with 10 mM P_i (P_i).Fold change for the phosphate treated groups was determined relative to control, which was set at 1 $p \leq 0.05$ (*), $p \leq 0.01$ (**), and $p \leq 0.001$ (***).

Table 3. Detection Pattern in MV of Genes Downregulated by P_i Using Mass Spectrometry

Gene	Detection in EV after 24h P_i exposure (17A)
Akp2	Present in all samples. *No significant alteration by Pi*
Phospho1	No detection
Pth1r	Cntrl –Medium EV Cntrl–ECM MV
Panx3	Present in all samples. *No significant alteration by P_i*
Slc13a5	Cntrl –Medium EV Cntrl–ECM MV
Cdsn	P_i –ECM MV

5.0 DISCUSSION

Recently, our lab has established that exposure to elevated P_i induces the release of matrix vesicles (MV) from both pre-odontoblast and vascular smooth muscle cells (Chaudhary, Kuzynski et al. 2016, Chaudhary, Khalid et al. 2018). Using mass spectrometric analysis, we determined that exposure to elevated P_i alters the composition of these vesicles (Figure 2) (Chaudhary, Khalid et al. 2018). In an unpublished RNA-seq analysis evaluating the effect of P_i on pre-odontoblast cells, we identified gene expression changes of many proteins involved in mineralization. The purpose of the present study was to determine if gene expression changes induced by elevated P_i contributed to alteration of MV composition.

While not the focus of the present investigation, we determined that P_i did not alter the size distribution of MV released from 17A cells. As size distributions are indications of vesicle type and therefore biogenesis pathway, this finding suggests that vesicles are generated through the same pathway even though their composition, and presumably function, are altered.

This study is the first to evaluate the relationship between gene expression and MV composition. We demonstrated significant changes in gene expression when 17A cells were exposed to elevated P_i over 72h. However, this did not appear to correlate with changes in the protein composition of the MVs (Figure 7, 8, 9, Table 2 and 3). This suggests that phosphate signaling, especially at the 24h time point, regulates protein processing and/or trafficking, which will direct relevant proteins into MV, separate from its action on gene expression.

However, this does not mean that gene expression changes do not contribute to the alteration of vesicle composition at later timepoints. Another possibility for why gene expression and alteration of protein composition do not show a correlation is that the timeframe used in this study to evaluate protein alteration may have been too short to determine the effects of gene expression changes. A longer, more comprehensive evaluation of MV composition and transcriptome analysis would need to be performed to determine if gene expression changes alter MV composition after longer exposure to elevated P_i.

Gene expression may also alter the composition of vesicles through alteration of the RNA composition of MV. EV are known to contain different types of RNA, including mRNA (György, Szabó et al. 2011, Yuana, Sturk et al. 2013, Zaborowski, Balaj et al. 2015, Rilla, Mustonen et al. 2017). Analysis of the proteins altered by P_i in MV released from pre-odontoblasts and vascular smooth muscles cells identified proteins involved in RNA processing overrepresented in proteins increased by P_i in MV (Figure 10). The alteration of these RNA processing proteins by P_i in MV may also indicate a change in MV nucleic acid composition. A way to evaluate this possibility would be to evaluate the nucleic acid composition of MV and compare that to total cell gene expression.

The MV samples used to evaluate changes in vesicle composition were most likely a heterogeneous EV population. In order to determine the purity of our samples, we implemented several quality control experiments: Cryo-EM, silver stain, and nanoparticle tracking analysis. We have determined that this collection mostly contains MV because of the size distribution profile and enrichment of TNAP (a protein enriched in MV). However, the collection most likely contains a small population of other types of EV as well. Most published evaluations of EV employ differential centrifugation to concentrate and partially purify vesicles. Generally, the

centrifugation steps include depletion of cellular debris then isolation of vesicles using greater than 100,000g speeds. The centrifugation speed can be calibrated to collect EV within a size range of interest. Using this method, we collected vesicles between 50nm and 220nm, and we confirmed our collection method by evaluating MV samples collected from MOVAS cells using Cryo-EM. However, these samples are still heterogeneous in nature (Thery, Amigorena et al. 2006).

Another method of EV isolation is size-exclusion chromatography. In this method, the EV are isolated based on size through a filter column. However, this method requires a pre-concentration step that may result in deformed EV or their rupture. This method will also result in different types of EV being present in the sample if they are in the same size range (Szatanek, Baran et al. 2015). Due to the heterogeneous nature of the sample preparation, there is a possibility that subtypes of MV are responsible for distinct functions: some to form hydroxyapatite, some to alter the ECM, and others to facilitate cell-cell communication (Witwer, Buzás et al. 2013). New techniques will need to be developed to better isolate and evaluate MV to determine more about their biogenesis and range of functions.

In this study, we evaluated the protein MV released from pre-odontoblastic cells. Other studies, however, have evaluated MV protein composition using osteoblasts or chondrocytes *in vitro* and cartilage tissue from an *in vivo* model. One group, for example, collected MV from femurs of chicken embryos, and while they identified many of the same proteins found in mouse osteoblast and chondrocyte MVs, they had different amounts present, indicating that it is important to consider the source when evaluating composition (Balcerzak, Malinowska et al. 2008).

Other studies have focused only on the composition of MV released from differentiating precursor cells without evaluating how the composition of MV may change. Our previous studies have shown that elevated P_i exposure not only stimulates MV release, but it also alters the composition of those MV. One group obtained MV from differentiating MC3T3-E1 cells and evaluated vesicles from both the ECM and the medium after 15 days of osteogenic differentiation. They identified many proteins involved in mineralization, such as TNAP. However, they did not fully address if there were differences between the medium and ECM groups.Instead, they assumed that the vesicles collected from both were the same (Xiao, Camalier et al. 2007) . The novelty of our previous studies in comparison to both these proteomic approaches is that we attempted to, and did, identify a MV release initiator (P_i). Using proteomic analysis, we were able to determine that vesicles released into the medium and ECM are different vesicles populations. Finally, we determined that P_i alters the composition of MV. These findings led us to wonder how P_i alters the composition of vesicles (Chaudhary, Kuzynski et al. 2016, Chaudhary, Khalid et al. 2018).

This present study is the first to evaluate a possible mechanism driving changes in MV composition released from osteogenic cells undergoing mineralization. By understanding the mechanism behind altered vesicle composition, we may be able to harness this understanding to develop new drug delivery or drug packaging methods. Future studies should employ a comprehensive and long-term evaluation of MV composition in comparison to gene expression to further elucidate a possible mechanism driving composition change and modulation of MV cargo.

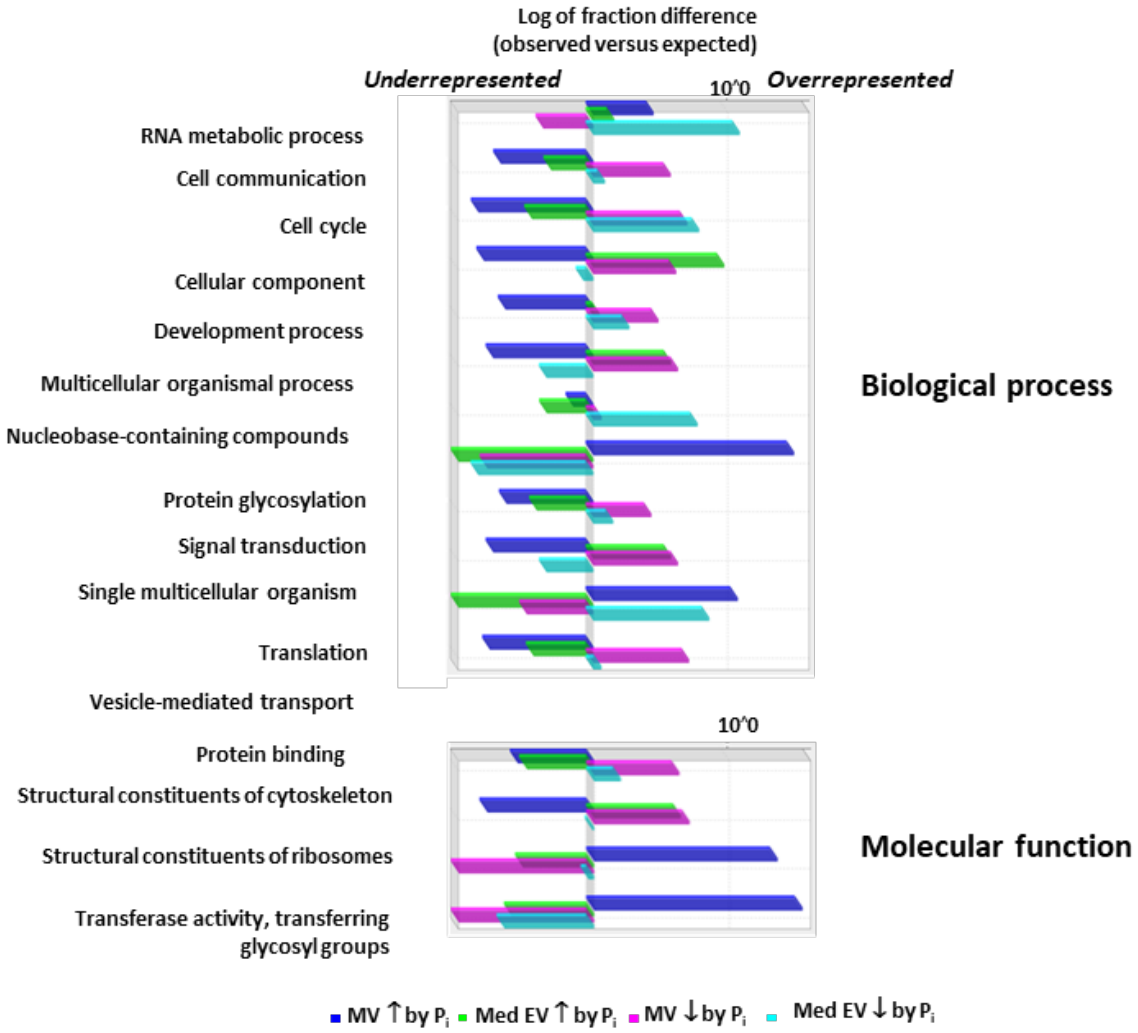

Figure 10. Protein profiling of EV released from 17IIA11 cells and altered by elevated phosphate.

EV released from 17IIA11 cells were collected under standard growth conditions (Ctrl) and upon 24h treatment with 10 mM Pi (Pi) both from conditioned medium (Med) and from the extracellular matrix (ECM). Bar chart of difference presenting the statistical overrepresentation test analysis results of proteins significantly changed by Pi (> 3-fold difference) and proteins present only in either Ctrl or in Pi group in annotation datasets of PANTHER GO-Slim for Biological process and molecular functions. All 1164 proteins identified by mass spectrometry were used as a reference. Statistically significant ($p<0.05$) results are shown.

6.0 CONCLUSIONS

In conclusion, this study demonstrated that while vesicle composition is altered due to P_i, MV size distribution is not altered. This indicates that the biogenesis pathway producing MV is unaltered by P_i, but the composition of the vesicles is affected. We attempted, for the first time, to determine a possible mechanism driving composition change in MV by P_i. From these studies, we have determined that gene expression changes are not responsible for changes in MV composition in the time frame evaluated (24h). This indicates that P_i signaling most likely influences trafficking and/or packaging of proteins separate from its influence on gene expression.

However, this does not mean that RNA expression changes do not alter the composition of vesicles. First, the transcriptome of MV may be altered or a longer evaluation period may be needed to determine if vesicle composition correlates to gene expression changes. Further studies evaluating MV composition over time will be required to investigate these possibilities.

BIBLIOGRAPHY

(2006). "Sodium phosphate." Cold Spring Harbor Protocols **2006**(1): pdb.rec8303.
Alves, R. D., M. Eijken, J. van de Peppel and J. P. van Leeuwen (2014). "Calcifying vascular smooth muscle cells and osteoblasts: independent cell types exhibiting extracellular matrix and biomineralization-related mimicries." BMC Genomics **15**(1): 965.
Anderson, H. C. (1967). "Electron microscopic studies of induced cartilage development and calcification." J Cell Biol **35**(1): 81-101.
Anderson, H. C., R. Garimella and S. E. Tague (2005). "The role of matrix vesicles in growth plate development and biomineralization." Front Biosci **10**(1): 822-837.
Balcerzak, M., A. Malinowska, C. Thouverey, A. Sekrecka, M. Dadlez, R. Buchet and S. Pikula (2008). "Proteome analysis of matrix vesicles isolated from femurs of chicken embryo." Proteomics **8**(1): 192-205.
Beck, G. R., Jr., E. Moran and N. Knecht (2003). "Inorganic phosphate regulates multiple genes during osteoblast differentiation, including Nrf2." Exp Cell Res **288**(2): 288-300.
Beck, G. R., Jr., B. Zerler and E. Moran (2000). "Phosphate is a specific signal for induction of osteopontin gene expression." Proc Natl Acad Sci U S A **97**(15): 8352-8357.
Bottini, M., S. Mebarek, K. L. Anderson, A. Strzelecka-Kiliszek, L. Bozycki, A. M. S. Simao, M. Bolean, P. Ciancaglini, J. B. Pikula, S. Pikula, D. Magne, N. Volkmann, D. Hanein, J. L. Millan and R. Buchet (2018). "Matrix vesicles from chondrocytes and osteoblasts: Their biogenesis, properties, functions and biomimetic models." Biochim Biophys Acta **1862**(3): 532-546.
Boyan, B. D., Z. Schwartz, L. D. Swain and A. Khare (1989). "Role of lipids in calcification of cartilage." Anat Rec **224**(2): 211-219.
Bradshaw, R. A. and E. A. Dennis (2010). Handbook of Cell Signaling, Elsevier/Academic Press.
Chaudhary, S. C., S. Khalid, V. Smethurst, D. Monier, J. Mobley, A. Huet, J. F. Conway and D. Napierala (2018). "Proteomic profiling of extracellular vesicles released from vascular smooth muscle cells during initiation of phosphate-induced mineralization." Connect Tissue Res **59**(sup1): 55-61.
Chaudhary, S. C., M. Kuzynski, M. Bottini, E. Beniash, T. Dokland, C. G. Mobley, M. C. Yadav, A. Poliard, O. Kellerman, J. L. Millán and D. Napierala (2016). "Phosphate induces formation of matrix vesicles during odontoblast-initiated mineralization in vitro." Matrix biology : journal of the International Society for Matrix Biology **52-54**: 284-300.
Chaudhary, S. C., M. Kuzynski, M. Bottini, E. Beniash, T. Dokland, C. G. Mobley, M. C. Yadav, A. Poliard, O. Kellermann, J. L. Millan and D. Napierala (2016). "Phosphate induces formation of matrix vesicles during odontoblast-initiated mineralization in vitro." Matrix Biol **52-54**: 284-300.

Cheloha, R. W., S. H. Gellman, J.-P. Vilardaga and T. J. Gardella (2015). "PTH receptor-1 signalling—mechanistic insights and therapeutic prospects." Nature reviews. Endocrinology **11**(12): 712-724.
Ciancaglini, P., M. C. Yadav, A. M. Simao, S. Narisawa, J. M. Pizauro, C. Farquharson, M. F. Hoylaerts and J. L. Millan (2010). "Kinetic analysis of substrate utilization by native and TNAP-, NPP1-, or PHOSPHO1-deficient matrix vesicles." J Bone Miner Res **25**(4): 716-723.
Colombo, M., G. Raposo and C. Théry (2014). "Biogenesis, Secretion, and Intercellular Interactions of Exosomes and Other Extracellular Vesicles." Annual Review of Cell and Developmental Biology **30**(1): 255-289.
Conrads, K. A., M. Yi, K. A. Simpson, D. A. Lucas, C. E. Camalier, L. R. Yu, T. D. Veenstra, R. M. Stephens, T. P. Conrads and G. R. Beck, Jr. (2005). "A combined proteome and microarray investigation of inorganic phosphate-induced pre-osteoblast cells." Mol Cell Proteomics **4**(9): 1284-1296.
Delorme, G., F. Saltel, E. Bonnelye, P. Jurdic and I. Machuca-Gayet (2005). "Expression and function of semaphorin 7A in bone cells." Biol Cell **97**(7): 589-597.
Fakhry, M., M. Roszkowska, A. Briolay, C. Bougault, A. Guignandon, J. I. Diaz-Hernandez, M. Diaz-Hernandez, S. Pikula, R. Buchet, E. Hamade, B. Badran, L. Bessueille and D. Magne (2017). "TNAP stimulates vascular smooth muscle cell trans-differentiation into chondrocytes through calcium deposition and BMP-2 activation: Possible implication in atherosclerotic plaque stability." Biochim Biophys Acta **1863**(3): 643-653.
Fan, Y., R. Bi, M. J. Densmore, T. Sato, T. Kobayashi, Q. Yuan, X. Zhou, R. G. Erben and B. Lanske (2016). "Parathyroid hormone 1 receptor is essential to induce FGF23 production and maintain systemic mineral ion homeostasis." The FASEB Journal **30**(1): 428-440.
György, B., T. G. Szabó, M. Pásztói, Z. Pál, P. Misják, B. Aradi, V. László, É. Pállinger, E. Pap, Á. Kittel, G. Nagy, A. Falus and E. I. Buzás (2011). "Membrane vesicles, current state-of-the-art: emerging role of extracellular vesicles." Cellular and Molecular Life Sciences **68**(16): 2667-2688.
Hasegawa, T. (2018). "Ultrastructure and biological function of matrix vesicles in bone mineralization." Histochem Cell Biol **149**(4): 289-304.
Huesa, C., D. Houston, T. Kiffer-Moreira, M. M Yadav, J. Luis Millan and C. Farquharson (2015). The Functional co-operativity of Tissue-Nonspecific Alkaline Phosphatase (TNAP) and PHOSPHO1 during initiation of Skeletal Mineralization.
Irizarry, A. R., G. Yan, Q. Zeng, J. Lucchesi, M. J. Hamang, Y. L. Ma and J. X. Rong (2017). "Defective enamel and bone development in sodium-dependent citrate transporter (NaCT) Slc13a5 deficient mice." PLoS One **12**(4): e0175465.
Ishikawa, M. and Y. Yamada (2017). "The Role of Pannexin 3 in Bone Biology." J Dent Res **96**(4): 372-379.
Julien, M., S. Khoshniat, A. Lacreusette, M. Gatius, A. Bozec, E. F. Wagner, Y. Wittrant, M. Masson, P. Weiss, L. Beck, D. Magne and J. Guicheux (2009). "Phosphate-dependent regulation of MGP in osteoblasts: role of ERK1/2 and Fra-1." J Bone Miner Res **24**(11): 1856-1868.
Khoshniat, S., A. Bourgine, M. Julien, P. Weiss, J. Guicheux and L. Beck (2011). "The emergence of phosphate as a specific signaling molecule in bone and other cell types in mammals." Cellular and Molecular Life Sciences **68**(2): 205-218.
Kim, H. J., T. Minashima, E. F. McCarthy, J. A. Winkles and T. Kirsch (2010). "Progressive ankylosis protein (ANK) in osteoblasts and osteoclasts controls bone formation and bone remodeling." J Bone Miner Res **25**(8): 1771-1783.

McKee, M. D. and A. Nanci (1996). "Osteopontin: an interfacial extracellular matrix protein in mineralized tissues." Connect Tissue Res **35**(1-4): 197-205.
Millan, J. L. (2013). "The role of phosphatases in the initiation of skeletal mineralization." Calcif Tissue Int **93**(4): 299-306.
Mitton, E., C. M. Gohr, M. T. McNally and A. K. Rosenthal (2009). "Articular cartilage vesicles contain RNA." Biochemical and biophysical research communications **388**(3): 533-538.
Oh, S.-K., J.-O. Shin, J.-I. Baek, J. Lee, J. W. Bae, H. Ankamerddy, M.-J. Kim, T.-L. Huh, Z.-Y. Ryoo, U.-K. Kim, J. Bok and K.-Y. Lee (2015). "Pannexin 3 is required for normal progression of skeletal development in vertebrates." The FASEB Journal **29**(11): 4473-4484.
R., B. G. (2003). "Inorganic phosphate as a signaling molecule in osteoblast differentiation." Journal of Cellular Biochemistry **90**(2): 234-243.
Rackov, G., N. Garcia-Romero, S. Esteban-Rubio, J. Carrión-Navarro, C. Belda-Iniesta and A. Ayuso-Sacido (2018). "Vesicle-mediated control of cell function: the role of extracellular matrix and microenvironment." Frontiers in Physiology **9**.
Rilla, K., A.-M. Mustonen, U. T. Arasu, K. Härkönen, J. Matilainen and P. Nieminen (2017). "Extracellular vesicles are integral and functional components of the extracellular matrix." Matrix Biology.
Roberts, S. J., A. J. Stewart, P. J. Sadler and C. Farquharson (2004). "Human PHOSPHO1 exhibits high specific phosphoethanolamine and phosphocholine phosphatase activities." Biochem J **382**(Pt 1): 59-65.
Rosenthal, A. K., C. M. Gohr, J. Ninomiya and B. T. Wakim (2011). "Proteomic analysis of articular cartilage vesicles from normal and osteoarthritic cartilage." Arthritis & Rheumatism **63**(2): 401-411.
Shapiro, I. M., W. J. Landis and M. V. Risbud (2015). "Matrix vesicles: Are they anchored exosomes?" Bone **79**: 29-36.
Szatanek, R., J. Baran, M. Siedlar and M. Baj-Krzyworzeka (2015). "Isolation of extracellular vesicles: Determining the correct approach (Review)." International Journal of Molecular Medicine **36**(1): 11-17.
Thery, C., S. Amigorena, G. Raposo and A. Clayton (2006). "Isolation and characterization of exosomes from cell culture supernatants and biological fluids." Curr Protoc Cell Biol **Chapter 3**: Unit 3 22.
Théry, C., M. Boussac, P. Véron, P. Ricciardi-Castagnoli, G. Raposo, J. Garin and S. Amigorena (2001). "Proteomic Analysis of Dendritic Cell-Derived Exosomes: A Secreted Subcellular Compartment Distinct from Apoptotic Vesicles." The Journal of Immunology **166**(12): 7309-7318.
Thouverey, C., A. Malinowska, M. Balcerzak, A. Strzelecka-Kiliszek, R. Buchet, M. Dadlez and S. Pikula (2011). "Proteomic characterization of biogenesis and functions of matrix vesicles released from mineralizing human osteoblast-like cells." J Proteomics **74**(7): 1123-1134.
Wang, S.-K., M. Choi, A. S. Richardson, B. M. Reid, B. P. Lin, S. J. Wang, J.-W. Kim, J. P. Simmer and J. C. C. Hu (2014). "ITGB6 loss-of-function mutations cause autosomal recessive amelogenesis imperfecta." Human Molecular Genetics **23**(8): 2157-2163.
Witwer, K. W., E. I. Buzás, L. T. Bemis, A. Bora, C. Lässer, J. Lötvall, E. N. Nolte-'t Hoen, M. G. Piper, S. Sivaraman, J. Skog, C. Théry, M. H. Wauben and F. Hochberg (2013). "Standardization of sample collection, isolation and analysis methods in extracellular vesicle research." Journal of Extracellular Vesicles **2**(1): 20360.

Wu, H., P.-N. Teng, T. Jayaraman, S. Onishi, J. Li, L. Bannon, H. Huang, J. Close and C. Sfeir (2011). "Dentin Matrix Protein 1 (DMP1) Signals via Cell Surface Integrin." The Journal of Biological Chemistry **286**(34): 29462-29469.
Wuthier, R. E. and G. F. Lipscomb (2011). "Matrix vesicles: structure, composition, formation and function in calcification." Front Biosci (Landmark Ed) **16**: 2812-2902.
Xiao, Z., C. E. Camalier, K. Nagashima, K. C. Chan, D. A. Lucas, M. J. de la Cruz, M. Gignac, S. Lockett, H. J. Issaq, T. D. Veenstra, T. P. Conrads and G. R. Beck, Jr. (2007). "Analysis of the extracellular matrix vesicle proteome in mineralizing osteoblasts." J Cell Physiol **210**(2): 325-335.
Yanez-Mo, M., P. R. Siljander, Z. Andreu, A. B. Zavec, F. E. Borras, E. I. Buzas, K. Buzas, E. Casal, F. Cappello, J. Carvalho, E. Colas, A. Cordeiro-da Silva, S. Fais, J. M. Falcon-Perez, I. M. Ghobrial, B. Giebel, M. Gimona, M. Graner, I. Gursel, M. Gursel, N. H. Heegaard, A. Hendrix, P. Kierulf, K. Kokubun, M. Kosanovic, V. Kralj-Iglic, E. M. Kramer-Albers, S. Laitinen, C. Lasser, T. Lener, E. Ligeti, A. Line, G. Lipps, A. Llorente, J. Lotvall, M. Mancek-Keber, A. Marcilla, M. Mittelbrunn, I. Nazarenko, E. N. Nolte-'t Hoen, T. A. Nyman, L. O'Driscoll, M. Olivan, C. Oliveira, E. Pallinger, H. A. Del Portillo, J. Reventos, M. Rigau, E. Rohde, M. Sammar, F. Sanchez-Madrid, N. Santarem, K. Schallmoser, M. S. Ostenfeld, W. Stoorvogel, R. Stukelj, S. G. Van der Grein, M. H. Vasconcelos, M. H. Wauben and O. De Wever (2015). "Biological properties of extracellular vesicles and their physiological functions." J Extracell Vesicles **4**: 27066.
Yuana, Y., A. Sturk and R. Nieuwland (2013). "Extracellular vesicles in physiological and pathological conditions." Blood Rev **27**(1): 31-39.
Zaborowski, M. P., L. Balaj, X. O. Breakefield and C. P. Lai (2015). "Extracellular Vesicles: Composition, Biological Relevance, and Methods of Study." BioScience **65**(8): 783-797.